

# Localization of the G Protein $\beta\gamma$ Complex in Living Cells During Chemotaxis

Tian Jin, Ning Zhang, Yu Long, Carole A. Parent, Peter N. Devreotes\*

Gradients of chemoattractants elicit signaling events at the leading edge of a cell even though chemoattractant receptors are uniformly distributed on the cell surface. In highly polarized *Dictyostelium discoideum* amoebas, membrane-associated  $\beta\gamma$  subunits of heterotrimeric guanine nucleotide-binding proteins (G proteins) were localized in a shallow anterior-posterior gradient. A uniformly applied chemoattractant generated binding sites for pleckstrin homology (PH) domains on the inner surface of the membrane in a pattern similar to that of the  $G\beta\gamma$  subunits. Loss of cell polarity resulted in uniform distribution of both the  $G\beta\gamma$  subunits and the sensitivity of PH domain recruitment. These observations indicate that  $G\beta\gamma$  subunits are not sufficiently localized to restrict signaling events to the leading edge but that their distribution may determine the relative chemotactic sensitivity of polarized cells.

Chemotactic cells can move up shallow chemoattractant gradients, indicating that they can compare and process extremely small differences in concentrations of extracellular stimuli (1). This behavior has been attributed to two characteristics of chemotactic cells. First, the cells have the ability, referred to as directional sens-

ing, to spatially localize the activation of G protein-linked signaling pathways (2). Translocation of the PH domain-containing proteins to the inner face of the plasma membrane is an early event that marks the directional response (3, 4). Second, chemotactic cells exhibit polarized sensitivity in which the leading edge is the most responsive region to chemoattractants, whereas the trailing end is least sensitive (5, 6). Higher concentrations of stimuli or longer times of exposure are required to elicit pseudopod formation at the rear than from the front. It has been proposed that component(s) of the recep-

tor-G protein system may accumulate at the front of polarized cells, accounting for increased responsiveness to chemoattractants at the anterior (5-8). However, observations of living cells indicate that chemoattractant receptors remain evenly distributed on the surface of highly polarized cells (9, 10). The  $G\beta\gamma$  complex is an essential component of the receptor-G protein system required for chemotaxis of leukocytes and *Dictyostelium discoideum* amoebas (11, 12). Chronic or stimulus-induced clustering of  $G\beta\gamma$  to the front surface of a cell could possibly contribute to directional sensing and/or polarized sensitivity. To investigate the molecular basis of these properties of chemotactic cells, we determined the distribution of a G protein  $\beta$  subunit in living cells during chemotaxis.

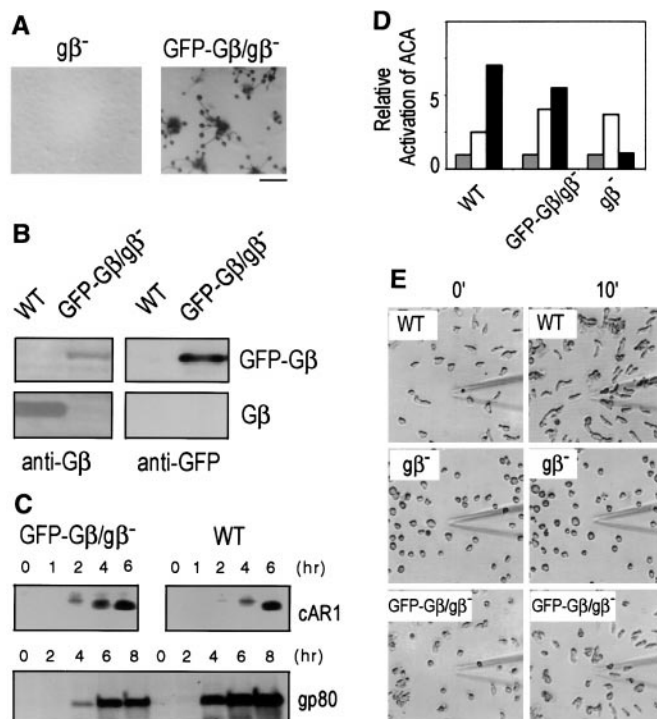
Green fluorescent protein (GFP) was fused to the  $NH_2$ -terminus of the unique  $G\beta$  subunit of *D. discoideum* (13). *D. discoideum* mutants that do not express the  $G\beta$  subunit ( $g\beta^-$  cells) are completely deficient in chemoattractant-induced responses and therefore are unable to aggregate and differentiate (12, 14). Stable expression of the GFP-tagged  $G\beta$  (GFP- $G\beta$ ) subunit rescued the chemotactic and developmental defects of the  $g\beta^-$  cells (Fig. 1) (15). Chemoattractant-induced expression of the early aggregation genes was similar to that of wild-type cells. Activation of adenylyl cyclase by guanosine 5'-O-(3'-thiotriphosphate) (GTP- $\gamma$ -S) in vitro was restored, and cyclic adenosine 3',5'-monophosphate (cAMP)-filled micropipettes induced equivalent chemotactic responses in wild-type and rescued cells.

The distribution of GFP- $G\beta$  in the rescued cells was determined during chemotaxis in the

Department of Biological Chemistry, Johns Hopkins University School of Medicine, Baltimore, MD 21205, USA.

\*To whom correspondence should be addressed. E-mail: pnd@welchlink.welch.jhu.edu

**Fig. 1.** GFP- $G\beta$  retains functions of the wild-type  $G\beta$ . (A) Developmental phenotype of GFP- $G\beta/g\beta^-$  cells. Cells were harvested from shaking cultures, washed, and plated on nonnutrient agar. Pictures were taken 36 hours after the cells were plated. Calibration bar is 2 mm. (B) Expression of GFP- $G\beta$  protein. Lysates of wild-type (WT) and GFP- $G\beta/g\beta^-$  cells were subjected to protein immunoblot analyses. An antibody to  $G\beta$  (anti- $G\beta$ ) detected a band of 40 kD, the size of the endogenous  $G\beta$ , in wild-type cells and a band of 70 kD, the predicted size of the fusion protein, in GFP- $G\beta/g\beta^-$  cells. An antibody to GFP (anti-GFP) recognized a band of 70 kD in GFP- $G\beta/g\beta^-$  cells and did not detect any bands in wild-type cells (15). (C) Induction of aggregative-gene expression in GFP- $G\beta/g\beta^-$  cells. GFP- $G\beta/g\beta^-$  and wild-type cells were stimulated with 100 nM cAMP at 6-min intervals for 6 hours. Cell samples were taken after the indicated incubation periods, and lysates were subjected to protein immunoblot analyses of the chemoattractant receptor, cAR1, and the adhesion glycoprotein, gp80 (25). (D) Activation of adenylyl cyclase (ACA). Adenylyl cyclase activity in lysates of wild-type, GFP- $G\beta/g\beta^-$ , and  $g\beta^-$  cells was measured in buffer (shaded bars), in the presence of  $Mn^{2+}$ , which measures unregulated intrinsic activity of the enzyme (open bars), and in the presence of GTP- $\gamma$ -S (black bars) as previously described (12). Mean values from an experiment done in duplicate are shown. At least one other independent experiment was performed for each cell line and yielded similar results. (E) Chemotaxis of the GFP- $G\beta/g\beta^-$  cells. Cells were allowed to differentiate to aggregation stage by stimulating them with cAMP for 7 hours. These cells were washed, placed on glass cover slides, and then examined for chemotactic response to cAMP in a micropipette assay. At time 0, a micropipette filled with 1  $\mu$ M cAMP was applied to the surface of the slide. The positions of the cells at time 0 and 10 min are shown. Widths of fields are 150  $\mu$ m.



## REPORTS

gradients formed by the micropipettes (Fig. 2). About 70% of the tagged G $\beta\gamma$  subunits were associated with the plasma membrane, and 30% remained in the cytosol (16). The fluorescent signals associated with the membrane were distributed in a shallow anterior-posterior gradient, with a higher concentration at the anterior end. When the micropipette was repositioned, the cells often turned their anterior ends toward the newly established chemoattractant gradient, indicating that these differentiated cells were highly polarized. The distribution of GFP-G $\beta$  was compared with that of the chemoattractant receptor for cAMP, cAR1, fused to GFP (cAR1-GFP). In contrast to the polarized distribution of GFP-G $\beta$ , the receptors were distributed uniformly along the cell surface (Fig. 3). As the cells were undergoing rapid morphological changes associated with chemotaxis, the polarized distribution of the membrane-associated GFP-G $\beta$  and the uniform distribution of cAR1-GFP were maintained (17).

Activation of G protein-linked signaling systems was visualized in living cells by monitoring the recruitment of a PH domain to binding sites on the inner face of the plasma membrane (3, 4). Recruitment of PH domain-containing proteins to the membrane is an indicator of relative sensitivity to the chemoattractant. Cells expressing the cytosolic regulator of adenylyl cyclase (CRAC) or its PH domain fused to GFP (CRAC-GFP or PH<sub>crac</sub>-GFP) were differentiated to the aggregation stage, when cells display strong morphological and behavioral polarity (6, 7). Before stimulation with cAMP, the PH<sub>crac</sub>-GFP fluorescent signal was distributed uniformly throughout the cytosol (18). When a low concentration of stimulus was uniformly applied, PH<sub>crac</sub>-GFP was preferentially recruited to the inner surface of the membrane at the anterior of the cell and was depleted from the cytosol in the posterior of the cell. Within seconds after stimulation, PH<sub>crac</sub>-GFP then diffused back to the cytosol throughout the entire cell (Fig. 4). Higher concentrations of chemoattractant resulted in a less pronounced asymmetric recruitment of PH<sub>crac</sub>-GFP. These observations suggest that the anterior region of a highly polarized cell displays a higher sensitivity to chemoattractant because there is a higher concentration of G $\beta\gamma$  subunits at the front.

To determine whether the asymmetric distribution of G $\beta\gamma$  subunits and generation of binding sites for PH domains depend on the actin cytoskeleton, we treated cells with latrunculin A, which inhibits actin polymerization (3, 19). During treatment, cells rapidly lost polarity and became rounded and immobile. Within minutes, the asymmetric distribution of GFP-G $\beta$  was no longer detected, and the protein was uniformly distributed along the plasma membrane and within the cytosol of the rounded cells (Fig. 4). Accordingly, when the latrunculin A-treated cells were stimulated with a uniformly applied low concentration of cAMP (10 nM),

binding sites for CRAC-GFP were generated along the entire cell perimeter (20). The immobilized cells were still capable of directional sensing, but sensitivity was now uniformly distributed. When the micropipette was moved around the cell, the distribution of GFP-G $\beta$  remained uniform, but CRAC-GFP translo-

cated to the region of the surface closest to the micropipette and followed the micropipette with time lag of about 10 s (Fig. 4).

The latrunculin A experiments suggest that the anterior-posterior distribution of G $\beta\gamma$  subunits depends on the intrinsic polarization of the cell and does not require prior exposure

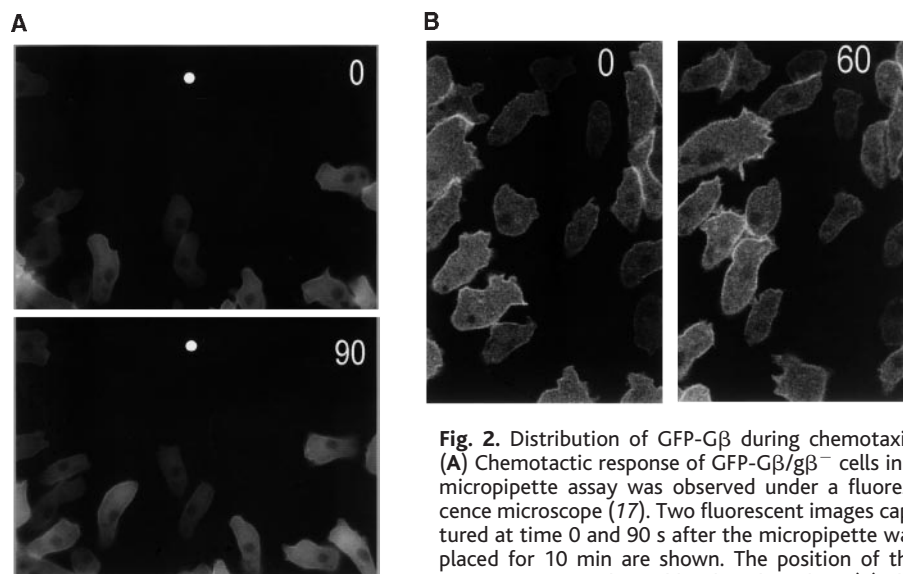


**Fig. 2.** Distribution of GFP-G $\beta$  during chemotaxis. (A) Chemotactic response of GFP-G $\beta$ /g $\beta$ <sup>-</sup> cells in a micropipette assay was observed under a fluorescence microscope (17). Two fluorescent images captured at time 0 and 90 s after the micropipette was placed for 10 min are shown. The position of the micropipette is indicated by the white dots. (B) The

chemotactic GFP-G $\beta$ /g $\beta$ <sup>-</sup> cells were observed under a confocal microscope (17). Two confocal fluorescent images captured at time 0 and 60 s after the micropipette was placed for 10 min are shown. The micropipette is located near the upper right corners of the images. Animated versions of these figures are available on *Science Online* (26).

**Fig. 3.** Quantitation of cellular distribution of GFP-G $\beta$  and cAR1-GFP in chemotactic cells. (A) Confocal images of GFP-G $\beta$  and cAR1-GFP in chemotaxing cells. A GFP-G $\beta$ /g $\beta$ <sup>-</sup> cell and a cAR1-GFP/car1<sup>-</sup> cell are chemotactically moving toward the upper middle of the frames (17). Distribution of GFP-G $\beta$  subunits and of cAR1-GFP is shown as intensity of the fluorescent signals. Color bar shows arbitrary intensity of fluorescence. a, b, c, and d represent points on the cell surface. Animated versions of this experiment are available on *Science Online* (26). (B) Quantitative analyses of the distribution of GFP-G $\beta$  and cAR1-GFP. Confocal fluorescent images were analyzed with a two-dimensional analysis program (Noran). Fluorescence intensities were measured along the lines a to c and b to d and plotted as a function of distance. Asymmetric distribution of fluorescent signals was observed in 18 out of 21 GFP-G $\beta$ /g $\beta$ <sup>-</sup> cells in a chemotaxis event, whereas the other three were not well polarized.

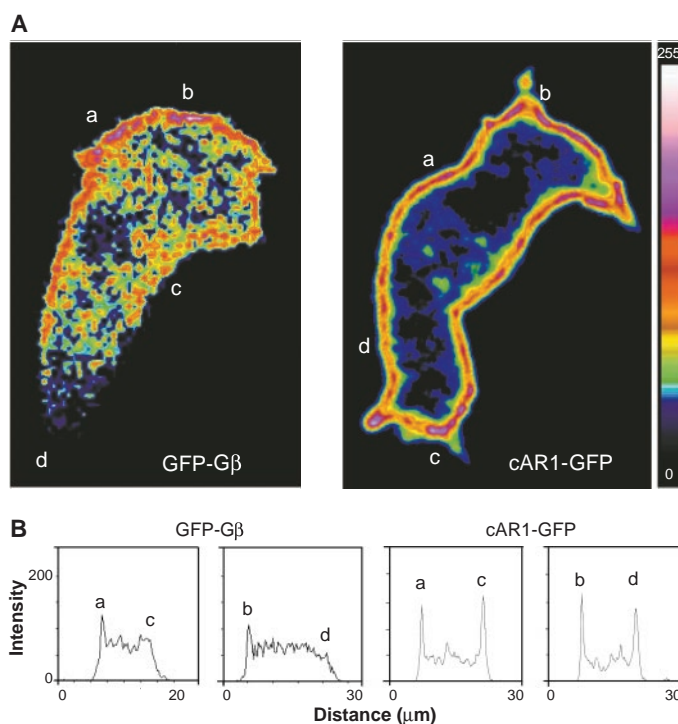
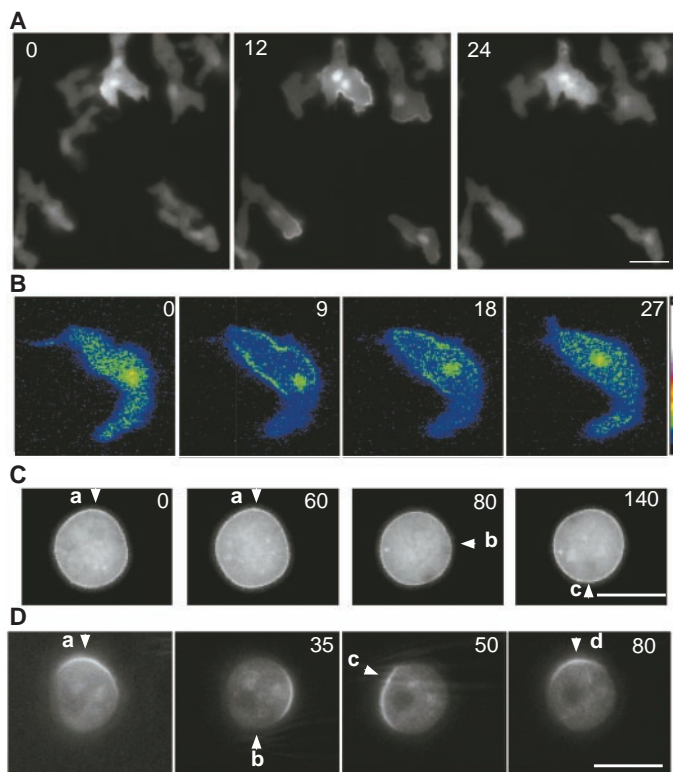


**Fig. 4.** Translocation of PH domains in cells. **(A)** Translocation of GFP-tagged PH domains to the anterior surface of polarized cells. cAMP (final concentration =  $10^{-6}$  M) was uniformly applied to polarized cells expressing PH<sub>crac</sub>-GFP, and the cells were observed by fluorescence microscopy. Numbers in the upper left corner are seconds after the addition of cAMP. In these frames, the fronts of the cells point to the lower right corner of the images. **(B)** A polarized cell was exposed to uniform concentration of cAMP (final concentration =  $10^{-6}$  M), and confocal fluorescence images of PH<sub>crac</sub>-GFP were captured at 3-s intervals. False color images were created as in Fig. 3. The front of the cell points to the upper left corner of the images. **(C)** A micropipette containing 1  $\mu$ M cAMP was placed next to a latrunculin A-treated GFP-G $\beta$ /g $\beta^{-}$  cell. As indicated by an arrow, the micropipette was placed at point a for 1 min and then moved to points b and c. **(D)** A micropipette containing 1  $\mu$ M cAMP was placed next to a latrunculin A-treated cell expressing CRAC-GFP. As indicated by an arrow, the micropipette was positioned at point a and then moved around the cell to points b, c, and d. For **(C)** and **(D)**, fluorescent images were captured every 5 s. Numbers in the upper right corners are seconds of selected frames. Calibration bars are 10  $\mu$ m. Animated versions of **(A)**, **(B)**, and **(D)** can be viewed on Science Online (26).



to chemoattractant gradients. However, chemoattractants were able to modulate the cellular axis. Although polarized cells often reoriented their anterior ends when micropipettes were repositioned to set up a gradient behind them, they sometimes collapsed their existing anterior ends and gradually reestablished polarity in the new direction. In these cases, the asymmetric distribution of G $\beta$  $\gamma$  also dissolved and reformed on the reversed axis of the cell.

These findings prompt us to amend local excitation/global inhibition models, which have been presented to explain how gradients elicit directional responses and chemotaxis (2, 21). In a gradient, local excitation at the cell anterior exceeds global inhibition that averages chemoattractant receptor occupancy along the entire cell, whereas at the posterior, inhibition exceeds excitation. To account for polarized sensitivity, we propose that local excitation depends on a combination of receptor occupancy and G protein concentration. With this stipulation, the regions of appearance of binding sites for PH domains mark the sites of future pseudopod formation rather than merely the direction of the gradient. This explains how uniform chemotactic stimuli that produce no gradient in

receptor occupancy can elicit directional responses as in chemokinesis (22). It also can explain how shallow gradients of chemoattractant elicit a response in the wrong direction if the combination of receptor occupancy and G protein concentration dominates on the side of the cell facing the lower concentration of chemoattractant. We note that when polarized cells are induced to turn by exposure to a new gradient, PH domains are recruited to the edge that leads cell movement rather than to the edge that faces the new gradient.

**References and Notes**

1. P. N. Devreotes and S. H. Zigmond, *Annu. Rev. Cell Biol.* **4**, 649 (1988); S. H. Zigmond, *J. Cell Biol.* **75**, 606 (1977).
2. C. A. Parent and P. N. Devreotes, *Science* **284**, 765 (1999).
3. C. Parent, B. J. Blacklock, W. M. Froehlich, D. B. Murphy, P. N. Devreotes, *Cell* **95**, 81 (1998).
4. R. Meili *et al.*, *EMBO J.* **18**, 2092 (1999).
5. S. H. Zigmond, H. I. Levitsky, B. J. Kreel, *J. Cell Biol.* **89**, 585 (1981).
6. J. A. Swanson and D. L. Taylor, *Cell* **28**, 225 (1982).
7. P. R. Fisher, R. Merkl, G. Gerisch, *J. Cell Biol.* **108**, 973 (1989).
8. F. Sanchez-Madrid and M. A. del Pozo, *EMBO J.* **18**, 501 (1999).
9. Z. Xiao, N. Zhang, D. B. Murphy, P. N. Devreotes, *J. Cell Biol.* **139**, 365 (1997).

10. G. Servant, O. D. Weiner, E. R. Neptune, J. W. Sedat, H. R. Bourne, *Mol. Biol. Cell* **10**, 1163 (1999).
11. D. E. Clapham and E. J. Neer, *Nature* **365**, 403 (1993); H. Arai, C. L. Tsou, I. F. Charo, *Proc. Natl. Acad. Sci. U.S.A.* **94**, 14495 (1997); E. R. Neptune and H. R. Bourne, *Proc. Natl. Acad. Sci. U.S.A.* **94**, 14489 (1997).
12. L. Wu, R. Valkema, P. J. Van Haastert, P. N. Devreotes, *J. Cell Biol.* **129**, 1667 (1995); T. Jin, M. Amzel, P. N. Devreotes, L. Wu, *Mol. Biol. Cell* **9**, 2949 (1998).
13. The coding region of GFP-G $\beta$  fusion protein was cloned into pMC 34, an extrachromosomal expression vector of *D. discoideum* (12). G $\beta$ -null cells (g $\beta^{-}$ ) cells were transformed, and individual G418-resistant clones were selected.
14. P. Lilly, L. Wu, D. L. Welker, P. N. Devreotes, *Genes Dev.* **7**, 986 (1993).
15. The following observations suggest that the GFP-G $\beta$  fusion protein is expressed at a level similar to that of the endogenous G $\beta$  in wild-type cells. First, comparison with known numbers of cAR1-GFP molecules indicated that there are about  $2 \times 10^5$  GFP-G $\beta$  molecules per cell. This is comparable to the number of endogenous G $\beta$  molecules estimated from purification of G $\beta$  $\gamma$  (between  $0.8 \times 10^5$  and  $4 \times 10^5$  per cell) (23). Second, previous studies have indicated that massive overexpression of G $\beta$  mRNA does not alter the level of the protein (24). The protein immunoblot analysis with the antibody to G $\beta$  may underestimate the level of GFP-G $\beta$  because the antibody is directed against the NH<sub>2</sub>-terminal fusion junction with GFP (14). The GFP-G $\beta$  appears to be fully functional during the aggregation stage because activation of adenylate cyclase and chemotactic responses are normal. The functions of the G $\beta$  in the later developmental stages are likely affected by the GFP fusion because multicellular morphogenesis is somewhat aberrant (25).
16. Subcellular fractionation and protein immunoblot analysis of lysates of wild-type cells showed that about 70% of G $\beta$  associates with the membrane fraction and the remainder presents in the cytosol (23). Thus, the endogenous G $\beta$  and GFP-G $\beta$  distribute similarly. Uniform stimulation of GFP-G $\beta$ /g $\beta^{-}$  cells with cAMP did not alter this ratio or change the distribution of the fluorescent signals.
17. Cells were prepared and observed with conventional and confocal microscopy as previously described (3, 9).
18. A fraction of PH<sub>crac</sub>-GFP localized in the nucleus, whereas CRAC-GFP localized exclusively in the cytosol. Nuclear PH<sub>crac</sub>-GFP did not redistribute. Other PH domains fused to GFP also localized in nuclei of mammalian cells [K. Venkateswarlu *et al.*, *Curr. Biol.* **8**, 463 (1998)].
19. I. Spector, N. Shochet, D. Blasberger, Y. Kashman, *Cell Motil. Cytoskeleton* **13**, 127 (1989).
20. An animated version of the redistribution of PH<sub>crac</sub>-GFP in response to a uniform increase of chemoattractant can be viewed in the supplemental materials (26).
21. H. Meinhardt, *J. Cell Sci.* **112**, 2867 (1999).
22. This effect may explain the reports of Varnum *et al.* (27), which showed that serial increments in uniformly applied chemoattractant increased the rate of random locomotion of *D. discoideum* amoebas. PH domains are selectively recruited to the leading edge of polarized neutrophils in response to uniform concentrations of chemoattractant (H. Bourne and G. Servant, personal communication).
23. N. Zhang and P. N. Devreotes, unpublished results.
24. U. Meng, C. J. Schmidt, F. Yi, D. J. Spring, E. J. Neer, *J. Biol. Chem.* **270**, 15892 (1995).
25. T. Jin *et al.*, *EMBO J.* **17**, 5076 (1998).
26. Supplemental material is available at [www.sciencemag.org/feature/data/1045235.shl](http://www.sciencemag.org/feature/data/1045235.shl).
27. B. J. Varnum-Finney, E. Voss, D. R. Soll, *Cell Motil. Cytoskeleton* **8**, 7 (1987); B. J. Varnum-Finney, K. B. Edwards, E. Voss, D. R. Soll, *Cell Motil. Cytoskeleton* **8**, 18 (1987).
28. We thank the members of our laboratory for help throughout the research and M. Delannoy for technical help with confocal microscopy analyses. NIH grant GM-28007 to P.N.D supported this work.

8 September 1999; accepted 20 December 1999